

Hybrid Technique in MRPID Controller for regulating Torque and Speed of BLDCM Drive System

K. Prathibanandhi¹, Research Scholar, College of Engineering Guindy, Anna University, Chennai, India, Prathiraj90@gmail.com

Dr. R. Ramesh², Associate Professor, Electrical and Electronics Engineering, Anna University, Chennai, India, rramesh@annauniv.edu

Abstract

The system proposed an ideal control computation based MRPID controller for the torque swell minimization of BLDC Motor drive framework. The control instrument incorporates two controlling circles to be specific, they are speed control circle and the torque control circle which are used to enhance the converter execution of BLDCM. For enhancing the control circle task, the MFO-RNN computation is proposed. Initially, the MFO is examined to improve the speed and inaccuracy of torque from the BLDCM framework. Utilizing the RNN procedure effectively, MFO computed value can be improved. The exemplary parameters are obtained for upgrading the task of MRPID controller. In light of the use of proposed calculation by direct the framework speed and limit the torque swells of BLDCM framework. The advantage of proposed strategy is powerful execution along with proliferated level of the quality and adaptability in unraveling the framework blunder. Furthermore the execution half breed procedure is actualized in the MATLAB/Simulink working stage and compared with existing strategies like ANFIS- Robust Neuro Fuzzy Inference System, Firefly Algorithm (FA) and MFO-RNN utilizing FOPID controller separately where the parameters like speed, current and torque ripple are reported.

Keywords: Brushless dc (BLDC) motor, Moth Flame Optimization (MFO), Recurrent Neural Network (RNN) algorithm, Multi Resolution

based PID (MRPID), torque ripple, speed and current

1. Introduction

Electric drives serve as an essential factor in Industrial plants with more than 5 billion engines constructed worldwide consistently. The standard private and business applications tend to utilize regular engine drive with single-stage enlistment or brushed dc engines inspite of their low proficiency and high maintenance [1]. A BLDCM are used in wide range of applications which includes medical, industrial and domestic applications without the presence of brush and commutator. It provides an effortless structure, extensive range of speed, high power, boundless torque with high expertise and great control over various speed range[2]. BLDCM is categorized into two unique featured classes, mounting surface lasting magnet in BLDC engines along with the interior perpetual magnet BLDCM [3]. The direction of speed is mandatory in the field of brushless DC engine drive for position control applications [4]. The value of speed exceeds in transient period and leads to a state of temporary inaction irrespective of consistent time frame [5]. The speed control framework applied is based on twofold circle is utilized in hardware for cars, home appliances, office computerization and accuracy in machines. The traditional control approaches which include non linear control and versatile control has been used for controlling the speed of BLDCM. The methodologies applied seem to be unpredictable and hard to execute [7].

The torque swell in existing BLDCM has been a setback for drive framework applications. The swell arises due to substitution in torque. The replacement torque applied to BLDCM diminishes the torque swell[8]. The various torque incorporated is activated by stator spaces with stator space as an interface. [9][10]. The prominent torque swell due to imperfect trapezoidal based emf waveform and its imperfections in compensating the stage current limits the application to provide high efficiency and dependability in events. The researches prove that there are no solutions for torque swell[11]. The occurrence of torque swell is due to high outbreak while exchanging the power gadgets and stator defects. It also arises when information supply voltage contains resonant parts and fluctuation in current[12][13]. This essentially requires the need of a productive controller to control the resonant exhibited with the information voltage for the engines and to eradicate the fluctuation in passage of current [14].

The torque swelling reduction for BLDCM was proposed in some research work. The proposed methodologies reduces the impact of torque, they are stage change strategy, hysteresis current technique, PWM strategy, current prescient control technique and torque control[16][17]. The speed of rotor and position data plays a vital role in BLDCM control approaches. Sensors are preferred to calculate the speed, position and estimation procedure[18]. The proposed Relative Integral(PI) for brushless DC engine takes enormous settling and arising time along with high motions in speed reaction[19]. Traditional methodologies adapted Genetic algorithms, PSO calculation, Neural Network and advanced slope plummet calculation[20].

2. Dynamic Strategy of BLDCM with Proposed Technique

The BLDCM operates on speed loop and torque loop, these loops are combined in the proposed hybrid methodology and evaluates minimum torque ripple value. The errors generated through speed and torque are optimized through multi objective functions.

The mathematical model is represented in equation below(1),

$$F_{S,T} = \text{Min}(e) = \min \left\{ \begin{array}{l} \alpha_{error} = \alpha_{ref} - \alpha \\ T_{error} = T_{ref} - T \end{array} \right\} \quad (1)$$

Here, $F_{S,T}$ is the objective function for speed error and torque ripple, e shows the value of error represents the error identified between the torque reference (T_{ref}) and generated value of the torque(T).

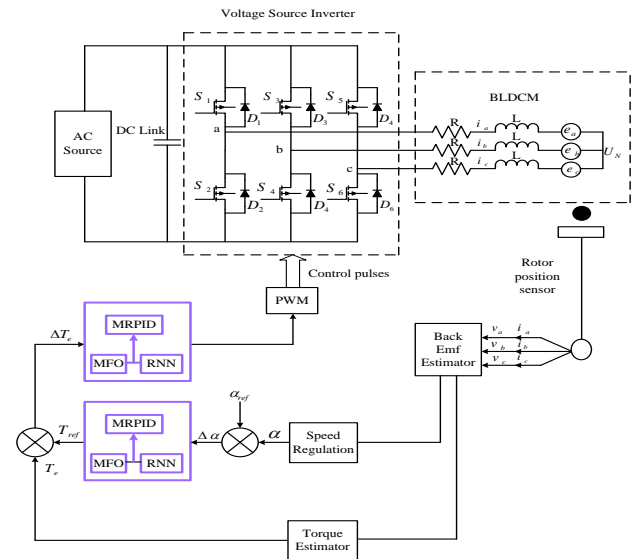


Figure 1: Modeling of the BLDCM and proposed control topology

In this section, the speed and torque characteristic of BLDCM is analyzed and determined the ripples. Before analyzing the characteristic of speed and torque, the modeling and controlling phases must be defined. In both phases, the phase and torque of the motor is controlled by utilizing wavelet based MRPID controller. Initially parameter of BLDCM is examined followed by control techniques. The BLDCM comprises of a power source in DC shape where the contribution of rectifier is obtained via AC supply and yield of the dc-interface voltage is provide for the VSI [26]. The DC control is rearranged according to the demand of BLDCM based proposed method. The replacement points are assured and obtained through rotor position. The generated Pulse Width Modulation (PWM) signals are obtained

from the speed direction and torque control arrangement of the BLDCM. The tolerability of the connected voltage is balanced by utilizing PWM method. The control flag is sustained by PWM hinder by balancing the VSI. The upcoming sections Presently, the numerical demonstrating of the BLDCM is clarified as following subsection.

2.1. Modeling of BLDCM

The DC voltage drives BLDCM and the current recompense is controlled by strong state switches. The replacement moves are dictated by rotor position. The Hall effect sensor detects the rotor shaft position representing the signs of various switches[27]. Whenever the rotor attractive shafts moves close to the hall sensors generating high or low flag values. They show either N or S post near the sensors. Fig1 below demonstrates the identical model of the BLDCM and its inverter [28]. A BLDCM comprises of three stator windings and lasting magnets on the rotor. Condition 2 depicted below holds the voltage condition of three windings along with the stage factors.

$$\begin{bmatrix} v_a \\ v_b \\ v_c \end{bmatrix} = \begin{bmatrix} i_a \\ i_b \\ i_c \end{bmatrix} \begin{bmatrix} R & 0 & 0 \\ 0 & R & 0 \\ 0 & 0 & R \end{bmatrix} + \left[\frac{d}{dt} \right] \begin{bmatrix} i_a \\ i_b \\ i_c \end{bmatrix} \begin{bmatrix} L & 0 & 0 \\ 0 & L & 0 \\ 0 & 0 & L \end{bmatrix} + \begin{bmatrix} e_a \\ e_b \\ e_c \end{bmatrix} + \begin{bmatrix} U_N \\ U_N \\ U_N \end{bmatrix} \quad (2)$$

Where, v_a, v_b and v_c represents the terminal phase voltages corresponding to the power ground, R provides the stator resistance of phase windings, i_a, i_b and i_c are phase current, L is the correlative inductance of the phase windings, e_a, e_b and e_c are trapezoidal back EMFs and U_N is the neural point to ground voltage respectively. The electromagnetic torque is calculated in the equation (3).

$$T_e = \left[\frac{i_a \cdot e_a + i_b \cdot e_b + i_c \cdot e_c}{\alpha} \right] \quad (3)$$

Here, α is the speed of the rotor. Since the rotor of a BLDCM is fixed magnet, the back EMFs are directly equivalent to the speed of

electricity in rotor which is calculated by the equation (4).

$$e_a = -e_b = k_e \cdot \alpha_r \quad (4)$$

Where, k_e is the back EMF coefficient and α_r is a fixed value (i.e. $\alpha_r = \frac{p\alpha}{2}$). According to equation (5) and (6), the speed of the motor can be calculated as following equation (5).

$$\alpha = \frac{u_{a,b} - 2(R \cdot i_a)}{pk_e} \quad (5)$$

The above equations are analyzed in the mathematical modeling of the BLDCM. The design of the speed controller has been explained as following section 3.1.

2.2. Design of speed controller

The speed controller's input applied voltage represents the back EMF output which is obtained when the stator flux communicates with the rotor flux. It is generated by a rotor magnet defining the speed and torque of the BLDCM. Initially the phase control of BLDCM is analyzed[29]. The speed controller proposed calculates the error speed value from the reference speed value (α_{ref}) to actual speed value. The proposed controller MRPID gives an optimal solution of pulses to decrease the torque ripple minimization of the BLDCM. The torque ripple elimination and error speed value reduced in the proposed controller that gives the solution of torque ripple minimization of the BLDCM. The gain parameter of wavelet based MRPID controller is optimized utilizing RNN technique. The values accomplished through gain parameters are evaluated for improving the process of tuning in the MFO. The process of optimization proposed is evaluated further to generate torque error value. The method proposed to reduces the torque ripples and error speed value through PWM to control the pulses.

2.3. Design of Torque estimator

For the propelled execution, accentuation ought to be set on the present swell concealment which will decrease the

electromagnetic torque swell in the meantime as indicated by condition (3). The swell is essentially generated out of replacement swell [30] and conduction district swell. During the occurrence of torque swell is obtained by three-stage inverter regulation, which can be diminished by proposed control methodology. The proposed instance torque control technique reduces the inductance level of BLDCM and resolves the imbalance among three stage windings. EMF unsettling influence and replacement torque remains consistent. Another sort of torque controller was Direct Torque Control (DTC) controller, which has basic structure and displayed speed torque reaction [31]. Here the torque estimator execution of reference torque error esteem is obtained through proposed phase controller and the real torque esteem is provided as the contribution of the comparator. During the progress blunder esteem is delivered, while the streamlining procedure is taken into consideration. The wavelet based MRPID controller and half and half strategy is enhanced to decrease the torque swells.

2.4. Control design of BLDCM based MRPID controller with a wavelet - A hybrid approach

In this section, minimization procedures for control structure in wavelet based MRPID controller is proposed. Figure 2 depicts the proposed controller based speed and torque estimator of BLDCM. The engine speed is perceived by observing the rotor position utilizing an ideal encoder mounted on the rotor shaft. The real and the charge speed distinction gives the comparing speed blunder esteems. At that point, the mistake and the adjustment in blunder esteems are given as a contribution to the DWT [32]. The blunder signals prepared through the multi wavelet change, it has three recurrence levels low, medium and high. Which is to complete two level disintegration of mistake flag in view of the recurrence as far as low and high recurrence blunder signals. Since there is more data of low and high recurrence with

multi wavelet decay than conventional wavelets, the blunder gets disintegrated to an abnormal state by utilizing the DWT.

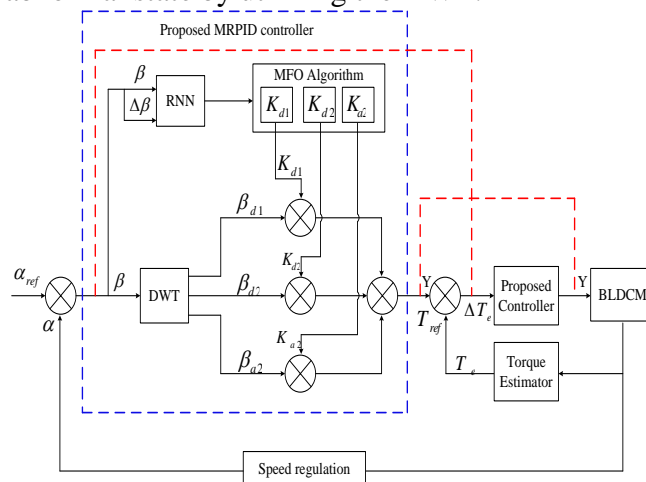


Figure.2: Proposed RNN- MFO based MRPID controller

The blunder co-proficient gets included RNN-MFO alongside the pick up parameters from the DWT to create the effective control speed and torque utilizing a MRPID controller. Be that as it may, the MFO calculation is connected to improve the pickup parameters of the RNN and are utilized for tuning the high, low and medium recurrence segments. In this way the control flag produced by the MRPID controller has been control the speed and torque of a BLDCM. In addition, the controller in view of MFO is employed to control the speed and torque of BLDCM in wide range and to give preferred execution over the regular RNN based controller. A proposition of PID controller with respect to the multi determination declining the errors by utilizing the wavelets. The deterioration in wavelets predetermines the customary PID history and its corresponding errors[33].The essential decomposition of MRPID controller representation through β is shown in following equation (6).

$$\beta = \sum \beta_i \text{ where, } i=1,2,\dots,n \quad (6)$$

Then a generalization of PID controller can be generated in following equation (7).

$$Y = \sum K_i \cdot \beta_i \quad (7)$$

Where, K_I shows controller parameters to be determined. The input of PID controller is error β that reflects on the error to obtain the control output Y as shown in equation (8).

$$Y_{PID} = K_P \beta(t) + K_I \int \beta(t) dt + K_D \left(\frac{d\beta(t)}{dt} \right) \quad (8)$$

Gains K_p, K_I and K_D are the extension of subordinate increases and utilizes the framework to monitor the errors separately. As far as recurrence data is considered, the corresponding vital terms tends to obtain the low-recurrence data of the blunder flag and subordinate captures the high-recurrence data of the mistake flag. On the off chance that more determination in recurrence is wanted, less determination in time is accomplished by utilizing a MRPID controller, in which the calculation time and many-sided quality has additionally been diminished. A MRPID controller disintegrates the blunder motion into its high, low recurrence signals, by applying multi wavelet deterioration to the mistake flag, the mistake gets decayed up to the second level of determination. At that point every last one of these segments is scaled by its particular pick up and after that additional together to produce the control flag is assessed in the condition (9).

$$Y_{MRPID} = K_{d1} \cdot \beta_{d1} + K_{d2} \cdot \beta_{d2} + K_{a2} \cdot \beta_{a2} \quad (9)$$

a MRPID can have at least two parameters one representing the quantity of disintegration levels performed on the blunder flag[34]. In the event that there is a one level decay next the blunder flag is named low and high recurrence flag and the controller has been containing just two pick up parameters. So as to achieve high determination two level disintegration of the blunder flag is performed, with the goal that age of three pick up parameters. Every one of these pick up parameters are embedded together with the blunder signs to deliver the viable control flag. The improvement procedure has been finished by utilizing the MRPID controller based half breed MFO-RNN, which is depicted in the accompanying section 3.

3. Hybrid Technique MFO-RNN technique for Gain Optimization

In the methodology proposed, partially the system has performed to control the parameter value raising up and generates core functionality for VSI in the BLDCM. The procedure of proposed control system is calculating the MFO for controlling the parameter value raising up. The computation of MFO generates the speed direction and torque estimator value. Speed direction and torque estimation is computed through MFO. The aim is to reduce the limit of blunder flag, direction of speed and torque estimation. Dataset holds the raising parameter value to monitor the progress of error. Control flag is raised by RNN while exchanging the circuit. The RNN procedure accomplishes the outcomes of MRPID controllers. The PWM flag is generated for the inverter at the EMF of the engine and control flag is obtained from RNN method. The RNN calculation efficiency is described in section 3.1.

3.1. Process involved in RNN training

The neural system is utilized to prove the recognition of cross breed framework. The obtained parameter is used for the proposed neural system. As depicted in figure 3, the contributions of RNN controller are the error signals ($\beta(t)$) and change in error signals ($\Delta\beta(t)$). The result of the RNN is fed as an input to the contribution of MRPID controller declared as Y . In order to accomplish the proficient control of the framework, the neural system has to be prepared for contributing for the controller to gather the necessary signals. The functionality of RNN is described in this. RNN is associated with the concealed neurons, which produces the framework of coordinated cycle.

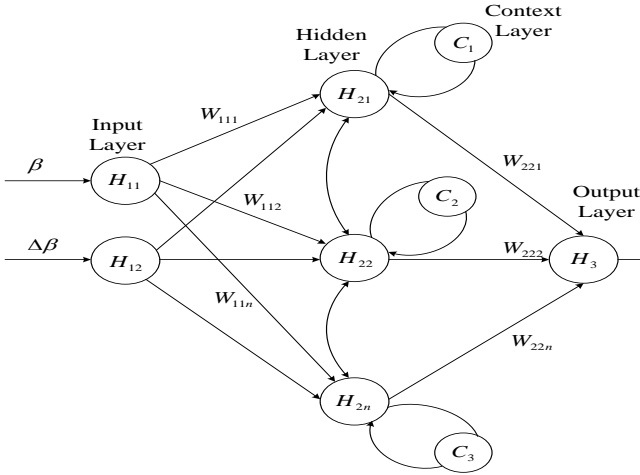


Figure 3: RNN based training structure

The input parameters involved in proposed RNN are speed error value (β), change error value ($\Delta\beta$) and count of hidden layers. RNN is utilized to form the cluster of the speed error value type whether the BLDCM is normal or irregular. Here, the input parameters are measured as the qualities and the network weight is allocated for input layer and fed into the hidden layer where it is forwarded to output layer respectively. The training algorithm steps are described as follows,

3.2 Steps for Training algorithm

Steps 1: Network dynamic

Step 1: In a RNN, the forward pass is not appropriate to MLP, apart from the initiations which pass through the hidden layer obtained in the previous step. Consider the length (T) as an input grouping X to a RNN with nodes as input, hidden and yield nodes. Let X_{tq} as the

estimation of contribution i at time t, a_j^t and b_j^t be the information and actuation to node j at time t separately. The initiation of the n-th hidden node is,

$$A_m = \sum_{n'=1}^N Wn'nb_n^{t-1} + \sum_{q=1}^Q W_{qn}X_{tq} \quad (10)$$

The differentiable activation for non linear function is applied as ilar to an MLP,,

$$b_n^t = \theta_n(a_{nt}) \quad (11)$$

The actuation work and b_n are the last enactment. The hidden initiation for predicting the estimation is performed utilizing t=2 initially, and consistently utilizing condition (10) and (11) with an addition of for each progression.

Step 2: The essential requirement for promoting the hidden node, i.e., b_i^0 should be selected, for comparing the system with the previous state and accepting any data from the information succession. The initial value is set to zero. The system contributions for generating the hub can be estimated as concealed initiations in the meantime using equation (12).

$$a_g^t = \sum_{n=1}^N w_{ng} \cdot b_n^t \quad (12)$$

The irregular associations are set at 1.0 for associating between the covered up and setting layers. The setting layer holds a duplicate of the past estimations corresponding to the hidden nodes.

Steps 2: Network learning

Step 1: The standard learning strategy utilized in RNN is the back spread calculation, which alters the arranged parameters in decreasing the inaccuracy with a slope plummet system. The increase in slope value increases generating negative error inclination is represented in the equation below(13).

$$\Delta w^n = -\alpha \cdot \left(\frac{\mathcal{G}L}{\mathcal{G}w^n} \right) \quad (13)$$

Where, Δw^n indicates the nth weight update, the loss factor is represented as L, w^n is the initial weight vector applied to Δw^n and $\alpha \in [0,1]$ is the learning rate. The learning iteration occurs recursively until a final criteria is met.

Step 2: The complication arises in the learning calculation which is obtained through nearest minimal value. Here the energy is excluded which results in isolation of algorithmic motion with respect to weight space. Using $p \in [0,1]$ as a momentum

parameter, this leads to increase in the convergence process and permits the learning algorithm to avoid from local minima, the equation is as follows,

$$\Delta w^n = p\Delta w^{n-1} - \alpha \cdot \left(\frac{\partial L}{\partial w^n} \right) \quad (14)$$

After the completion of the process, the RNN is categorizes the fault based signals . For improving the performance of RNN, MFO optimization algorithm is used for process verification . The RNN process depends on the forward and backward pass until the fault decreases to a lowest value if it fails the process is repeated. The working of MFO optimization algorithm is defined in following section.

3.3. Gain parameter optimization using MFO algorithm

The MFO is one of the current meta-heuristic advancement procedures. MFO calculation emulates the route strategy for moths in the night. In this assumption based calculation , the moths are the expected arrangements and the moths' positions represent the issue parameters [37]. The proposed system generates, moth flies with a fixed point as for the moon. During the process when moths visualize a man made simulated light, they attempt to fix flexible edge along with the vision to fly in a sheer line. The numerical model for the MFO depends on two parts, moth and fire [38]. The moths are original reference for specialists who travel around the inquiry space, the flares remain as the best position of moths that rises until a point. The work proves that the motivation of this calculation is the transverse orientation. According to this paper, MFO algorithm is utilized for optimizing the multi objective functions. Here the speed and torque error values are fed as an input of the each proposed system. Additionally the objective function which belongs to the fitness function is minimized. By minimizing the fitness function we obtain the optimal parameters of MRPID controllers. The

proposed MFO algorithm stepwise procedure is presented below.

Step 1: Parameters setting

Initially, the MRPID controller parameters are initiated randomly such as, K^{d1} , K^{d2} and K^{a2} respectively. The essential parameters of MFO incorporates, haphazardly create introductory populace for moths and flares with measurements, the quantity of factors, the most extreme cycle number. Indicate the irregular age of upper bound ($LB = [(LB)_1, (LB)_2, \dots, (LB)_{n-1}, (LB)_n]$) and lower bound ($UB = [(UB)_1, (UB)_2, \dots, (UB)_{n-1}, (UB)_n]$) of each variable.

Step 2: Position initialization

The situation of moths (M) and flames (F) are shown as conditions (22) and (23) separately. Every moth and fire can fly in various measurements in space by setting number of factors for every moth and flame.

$$\ddot{M} = \begin{bmatrix} \ddot{m}_{1,1} & \ddot{m}_{1,2} & \dots & \ddot{m}_{1,D} \\ \ddot{m}_{2,1} & \ddot{m}_{2,2} & \dots & \ddot{m}_{2,D} \\ \cdot & \cdot & \cdot & \cdot \\ \cdot & \cdot & \cdot & \cdot \\ \ddot{m}_{n,1} & \ddot{m}_{n,2} & \dots & \ddot{m}_{n,D} \end{bmatrix} \quad (15)$$

$$\ddot{F} = \begin{bmatrix} \ddot{f}_{1,1} & \ddot{f}_{1,2} & \dots & \ddot{f}_{1,D} \\ \ddot{f}_{2,1} & \ddot{f}_{2,2} & \dots & \ddot{f}_{2,D} \\ \cdot & \cdot & \cdot & \cdot \\ \cdot & \cdot & \cdot & \cdot \\ \ddot{f}_{n,1} & \ddot{f}_{n,2} & \dots & \ddot{f}_{n,D} \end{bmatrix} \quad (16)$$

Where, the position grid of moths is represented as \ddot{M} , \ddot{F} is the position lattice of flames, n identifies the quantity of moths and the quantity depending on dimensions are D the quantity. The

mathematical model of M and F can be ascertained by,

$$\hat{M}_i \circ \text{rand}(\hat{F}_i) = (UB_i - LB_i) \cdot \text{rand}() + LB_i \quad (17)$$

Where, \hat{M}_i and \hat{F}_i are the values belonging of the i^{th} column of the declared matrix \ddot{M} and \ddot{F} respectively. *rand* is defined as the random number generated through uniform distribution between the interval [0,1] and UB_i and LB_i values are the upper bound and lower bound of i^{th} variable respectively.

Step 3: Fitness value selection

Each flame is assessed generating a fitness function for obtaining the fitness values. There are contributed during the streamlining and the generated matrix is utilized to occupy the fitness functions related to their estimations of every moths and flames.

$$\ddot{M}^{of} = \left[\ddot{M}_{11}^{of}, \ddot{M}_{21}^{of}, \ddot{M}_{31}^{of}, \dots, \ddot{M}_{n1}^{of} \right] \text{ and} \\ \ddot{F}^{of} = \left[\ddot{F}_{11}^{of}, \ddot{F}_{21}^{of}, \ddot{F}_{31}^{of}, \dots, \ddot{F}_{n1}^{of} \right] \quad (18)$$

Based on the above function, the good fitness function is evaluated by the equation shown as follow.

$$\ddot{F}_{ff} = \text{Min } \beta(\psi) \quad (19)$$

Where, the mean of fitness function (\ddot{F}_{ff}) is minimize the error value of torque and speed ($\beta(\psi)$) in BLDCM drive system.

Step 4: Iteration start

In order to achieve the expected outcome numerical demonstrations are conducted for of merging towards the light, and the logarithmic winding is featured for MFO calculation in recreating the winding moving away of moths as for the flame,

$$\ddot{M}_i = S(\ddot{M}_x, \ddot{F}_y) = e^{bt} \cdot \cos(2\pi) \cdot D_x \cdot \ddot{F}_y \quad (20)$$

Where, $D_x = \left| \ddot{F}_y - \ddot{M}_x \right|$, \ddot{M}_x denotes the x^{th} moth, \ddot{F}_y represents the y^{th} flame. D_x is the gap between the x^{th} moth and y^{th} flame, b is the fixed value, t is the indiscriminate value between -1 and 1. Equation (20) rejuvenate the positions and expects the moths to act around the flame, which causes the MFO algorithm to be combined in neighborhood optima rapidly. In order to maintain a strategic distance from neighborhood ideal stagnation, every moth is obliged to refresh its situation as indicated, in a single of the flames in Equation (20). Every emphasis and in the wake of refreshing the rundown of flames, the flames are arranged in light of their wellness esteems. During that period the moths refresh their situations concerning their relating flames.

Step 5: Efficiency in result selection

The target flame values can be refreshed if any of the moths fits into the exact position. At the point when the cycle foundation is achieved, the best arrangement would be returned as the best obtained estimate of the ideal. During that point the resultant estimation of MFO calculation is improved by utilizing the proposed RNN strategy. With respect to the fitness work, the RNN is ideally prepared and produces an ideal yields and the equal contrast of the error estimations of the system is processed. Considering light of the half and half method, entire prepared systems are accomplished from the yield of system process. To ensure its characterization execution of the proposed framework depends on the accuracy of the framework, which is portrayed and execution is given in upcoming sections.

4. Results and Discussion

The efficiency of the partial calculation in proposed system is based on MRPID controller for limiting the torque swells in BLDCM drive framework. The aim is to ensure that the proposed BLDCM drive framework is actualized by MATLAB/Simulink stage. The result of

reproduction after applying the proposed system is compared and analyzed with the current strategies which includes FOPID controller based MFO-RNN . The improvement procedure is done by utilizing the proposed half and half MFO-RNN calculation in view of the multi-target work. The BLDCM test demonstrate is used for testing the proposed strategy and the framework parameters are indicated in table 1. The Simulink chart of the proposed architecture in presence of BLDCM is shown in the figure.4, where the torque swell disappears in the torque swell of the BLDCM drive framework in the half breed methodology . During the process, MRPID controller is employed for transition in phase of the BLDCM drive framework. Here, the proposed half breed method decreases the torque swell and maintains an efficient speed in the BLDCM framework. The restricting parameters are obtained initially from the BLDCM features including current, emf and speed . An analysis is done on the MRPID controller which is tuned at various conditions and the efficiency in variation of BLDCM system . The parameters involved in the proposed method is evaluated in the below section.

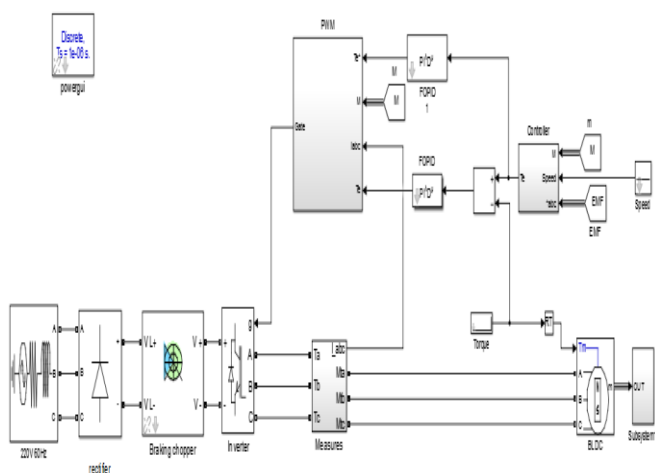


Figure 4: Simulation diagram of BLDCM proposed model

Table 1: Implementation parameters of BLDCM

Description	Values
Resistance of Stator phase (Rs)	0.2 (ohm)
Inductance in Stator phase (Ls)	8.5e-3
Linkage in flux	0.175
Back EMF flat area	120 (degrees)
Inertia	0.089 J(kg.m ²)
Frequency	60(Hz)
Source resistance	0.02 (ohm)
Source induction	0.05 e-3(H)

4.1. Performance analysis:

The operation of a proposed controller is to optimize the error function. The proposed algorithm optimizes the gain parameters, for minimizing the speed and torque errors. The minimized torque and the speed output are obtained with optimal tuning of gain parameters. The BLDCM drive is tested under constant speed conditions and constant torque conditions. Regarding the speed condition and torque condition, the performance of proposed controller action is tested under three cases conditions. Three cases are identified in the speed of the BLDCM which incorporates low speed, medium speed and high speed . The performance evaluation of three scenarios are

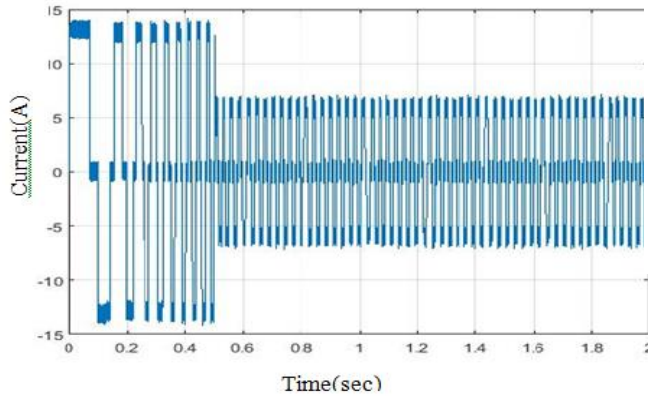
Case 1: Interpretation of attainment level of low speed

Case 2: Interpretation of attainment level of medium speed .

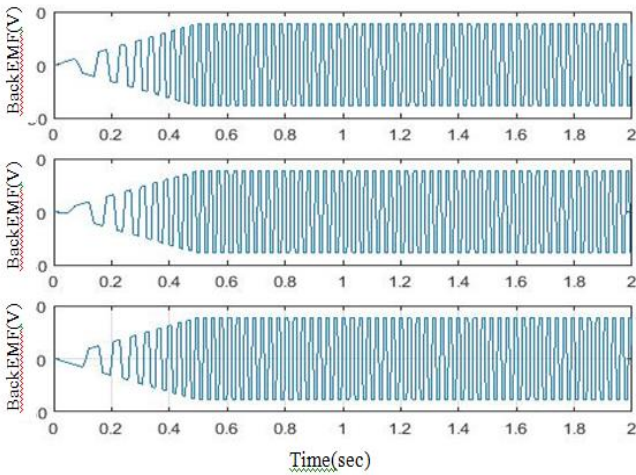
Case 3: Interpretation of attainment level of high speed In the following, these three cases are described and the performance of proposed method is described in below.

Case 1: Interpretation of attainment level of low speed , Here interpretation of the current, back EMF, speed and torque performances of BLDCM is considered for further analysis. The motor unloaded speed reference for drive response is demonstrated. The proposed MRPID controller, satisfies the K_p , K_i and K_d ,

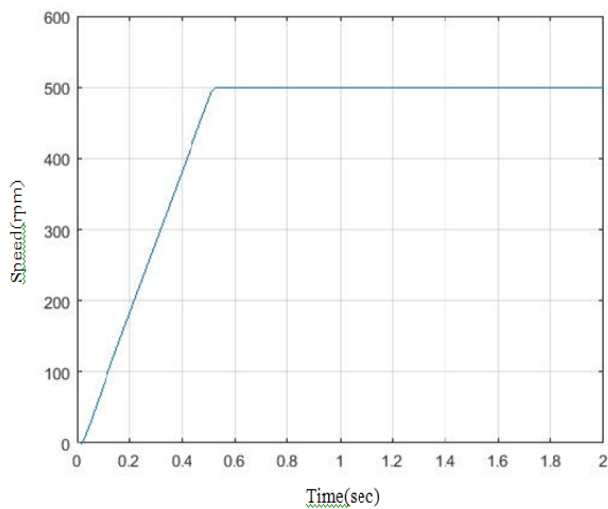
parameters to achieve minimal speed oscillations. The simulation process of the corresponding parameters are identified to be effective. The input current and back EMF has been illustrated in the figure 5 respectively.



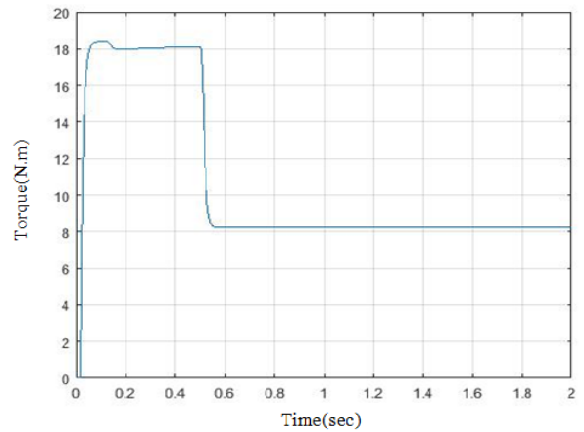
(a)



(b)

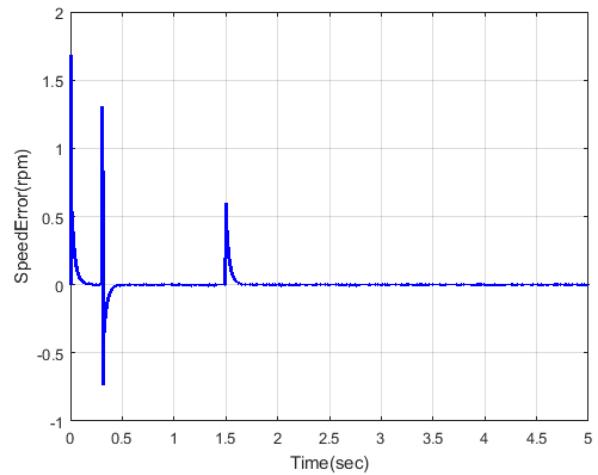


(c)

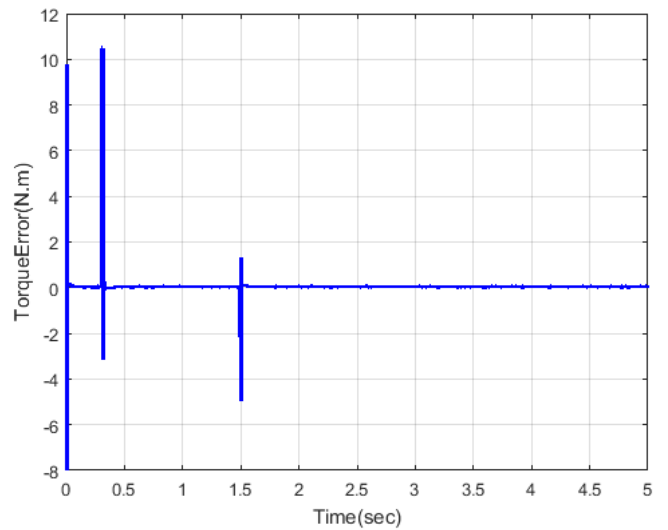


(d)

Figure 5: Performance analysis of case-1 (a) current, (b) back EMF, (c) speed and (d) torque



(a)

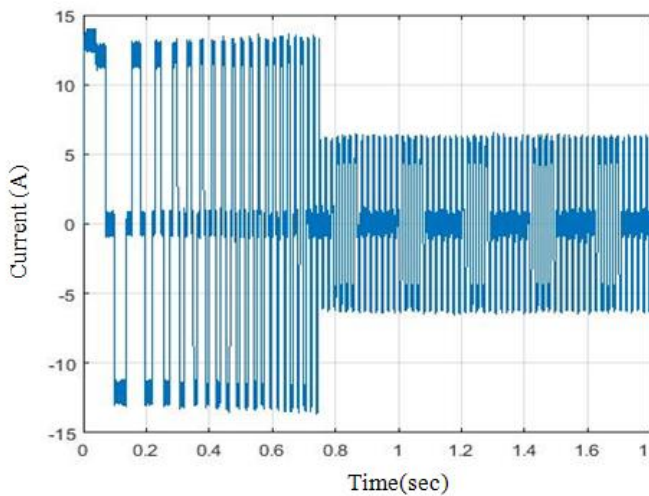


(b)

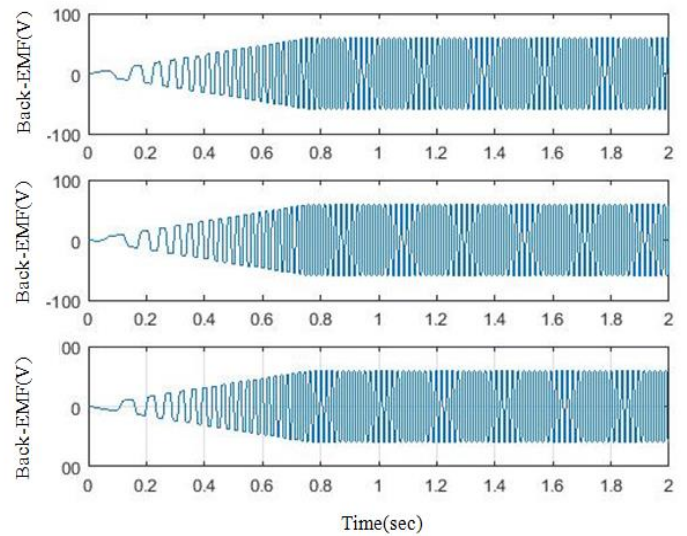
Figure 6: Interpretation of attainment level error values in case-1 (a) speed and (b) torque

In the figure 6 (a and b), the illustration of performance analysis of error value of the speed and torque has been depicted. The estimation differs with antecedent speed to the contemporary speed values of the proposed system. The performance analysis is captured with the speed and torque reference for ensuring the efficiency compared to the minimal small speed and torque level. By using proposed method, the output torque is firstly starts at zero and reach 8 Nm, finally torque is takes 1.5 seconds and reach 13 Nm respectively. Controlling the speed and minimization of torque ripple output performance of the proposed methodology has been competent over the other methodologies.

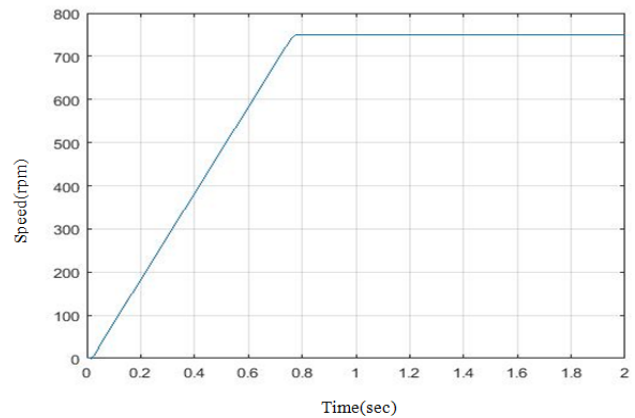
Case 2: Interpretation of attainment level of medium speed here the ripple minimization performance is analyzed with parameters of input current and back EMF and its corresponding parameters are predicted and illustrated in figure 7. In the figure 8, performance analysis of the error values are evaluated for proposed technique has been illustrated. The motor tracks the speed reference with minimal value of speed error for increased pace operation and standard error is minimized. The error value is found to be minimal as per the proposed technique which results in minimization of the ripple in emf from the BLDCM pace and torque.



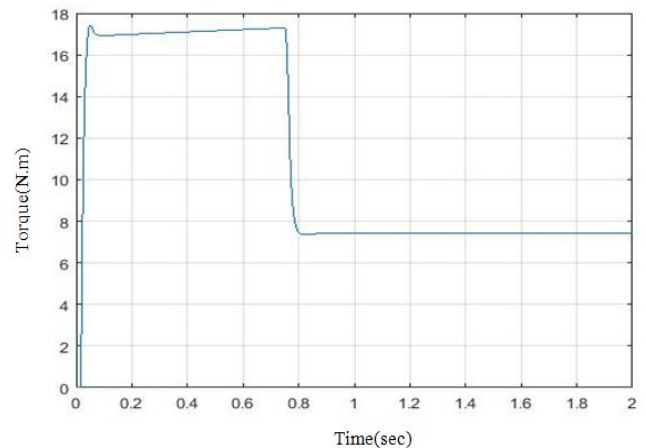
(a)



(b)

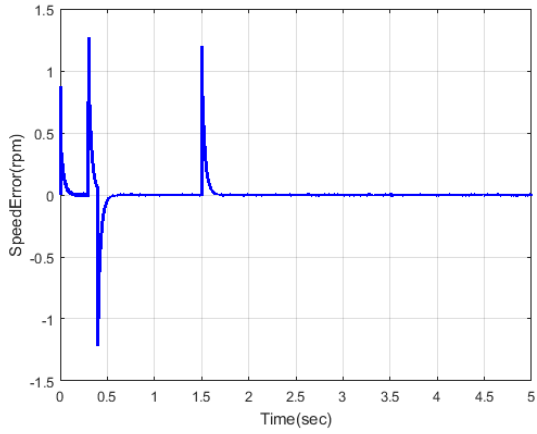


(c)

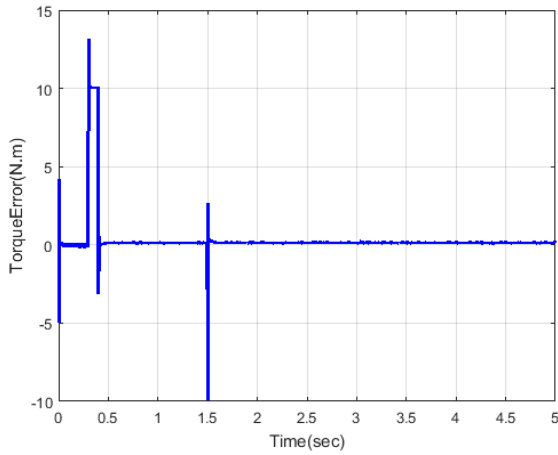


(d)

Figure 7: Performance analysis of (a) current, (b) back EMF, (c) speed, (d) torque in case 2



(a)



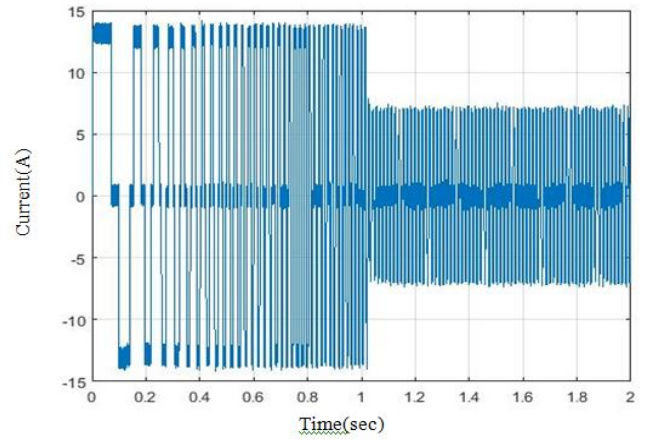
(b)

Figure 8: Performance analysis error values in case-2 (a) speed and (b) torque

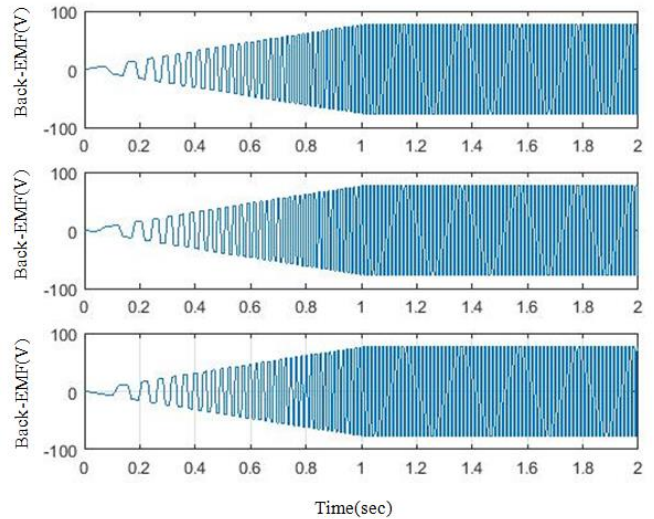
Here the proposed technique using MRPID controller takes the constant of 750 rpm speed of the motor, rise time is zero, 0.45 seconds settling process and without peak value. Then the settling time and peak value are analyzed, where the existing technique such as ANFIS with FA and MFO with RNN based FOPID controller kept peak value is 0.7 seconds, 0.42 seconds and settling time is 0.9 seconds and 0.45 seconds respectively.

Case 3: Interpretation of attainment level of High speed , The verifying process of dynamic performance in the BLDCM is achieved through high speed. The figure 9 represents the input current and back EMF motor with reference to high speed consisting of 1000 rpm .since it fails to maintain its consistency in controlling the input parameters of the BLDCM and pertained

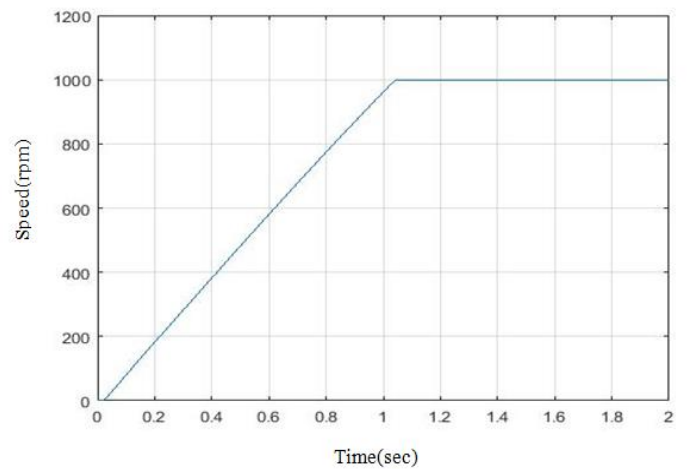
to the incoming current along with the speed regulation.



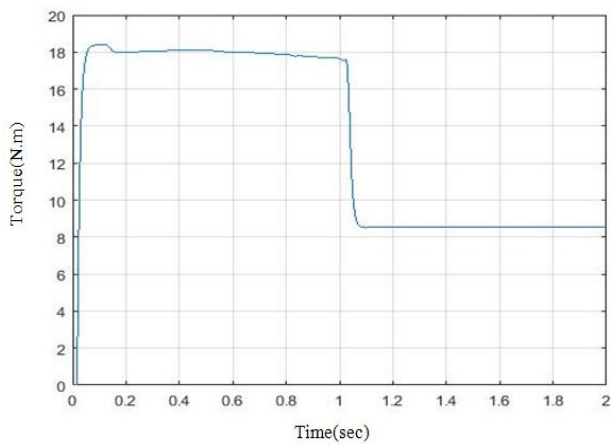
(a)



(b)

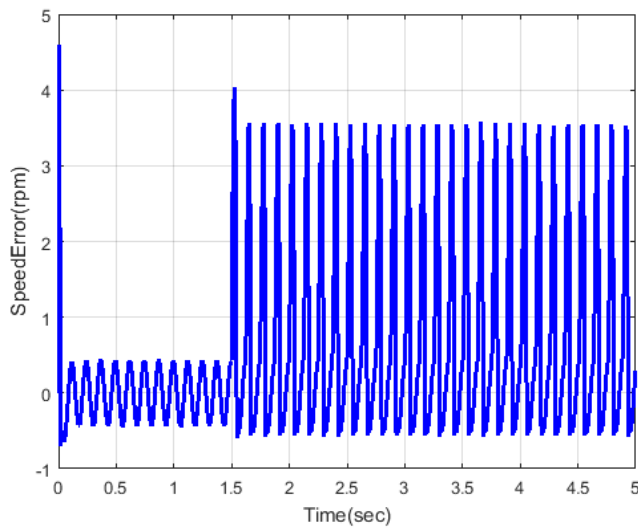


(c)

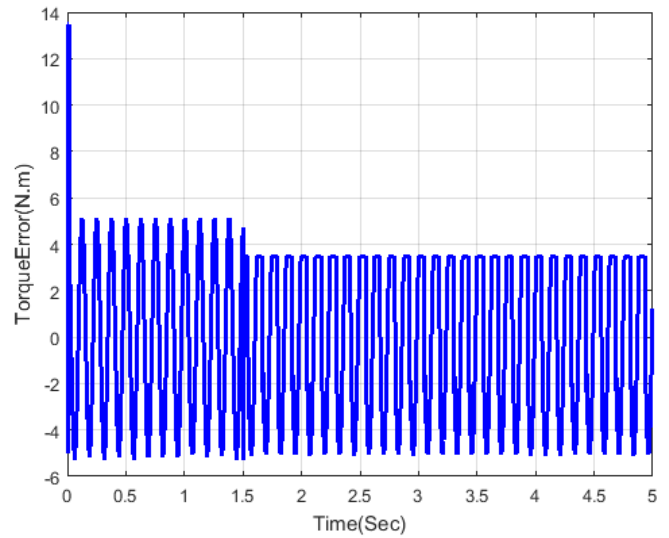


(c)

Figure 9: Interpretation of evaluation of (a) current, (b) back EMF, (c) speed and (d) torque estimation in case 3



(a)



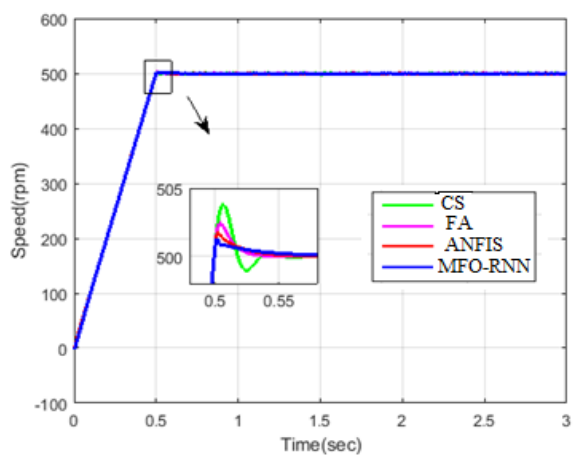
(b)

Figure 10: Evaluation of (a) speed and (b) torque error values in case 3

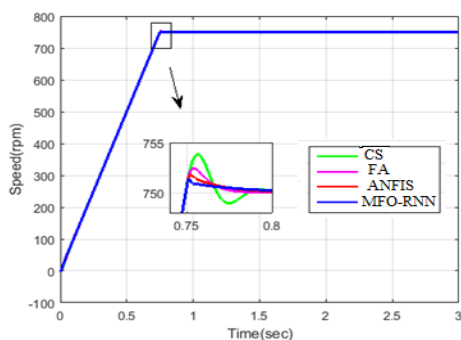
In the figure 10 (a) and (b) shows the performance analysis of speed and torque error values are evaluated. The speed error values and torque error values are reduced by using the proposed technique. Therefore the ripples in torque can be minimized in proposed methodology effectively when compared to than existing methods. The proposed strategy proves its stability for originating the minimal values of ripples in torque by linking with the traditional procedure. The analysis and contradictions of the proposed technique with the modern approaches prove an substantial illustrations in controlling the speed of BLDCM computation.

5. COMPARISON ANALYSIS OF THE PROPOSED TECHNIQUE

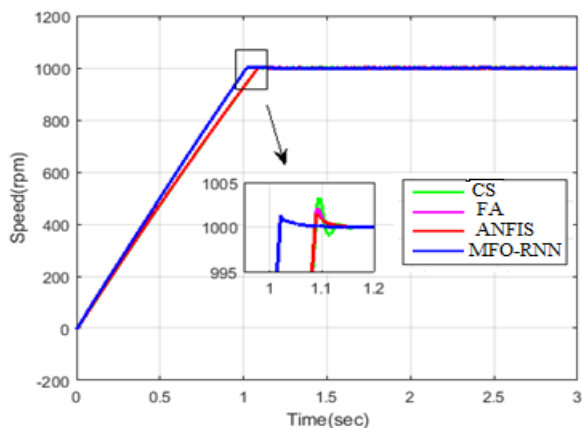
From the performance analysis the proposed methods is compared with the existing way of the torque and speed of BLDC motor. In this comparison analysis the 3 methods based on speed is shown in the figure 11. The time period 1.5 sec to 1.54 sec the oscillation is occurred based on this the proposed method is better than all 3 methods.



(a)

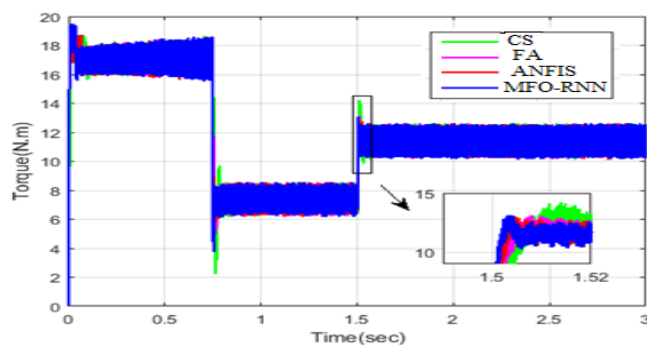


(b)

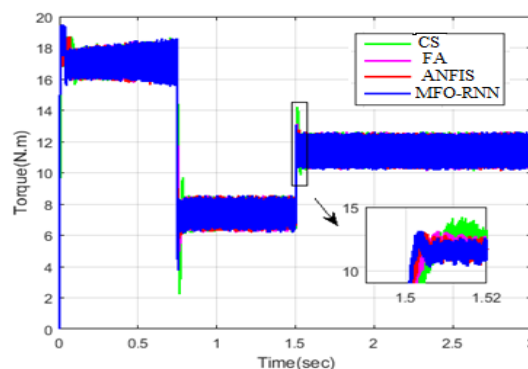


(c)

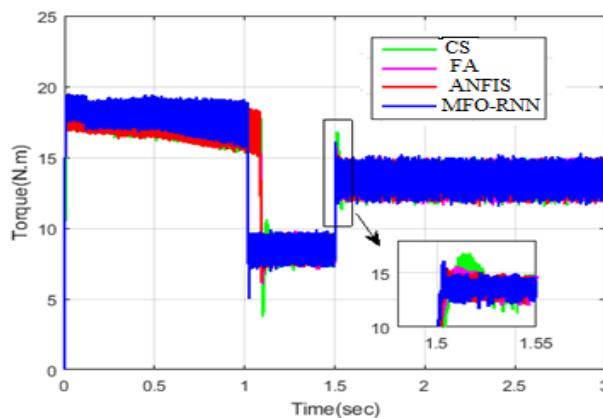
Figure.11: The comparison analysis of speed in (a) case1, (b) case2 and (c) case 3



(a)



(b)



(c)

Figure.12: The comparison analysis of torque in (a) case1, (b) case2 and (c) case 3

The speed of the BLDC motor proposed is compared and analyzed with existing methods. Input delimits in the motor depends on the input of the motor for controlling the torque based BLDC motor. Fig 11 compares the proposed methodology with existing methods, to elaborate the proposed method speed at three different cases(Case 1, 2 and 3). The assumed time is from 0.5 sec to 1 sec.

The overall analysis presented shows the speed and torque of the proposed BLDC at various levels of speed. The method proposed produces reduced speed ripple and determines its uniqueness. The obtained test run result keeps in track of the speed with corresponding reference speed. Fig 11 and 12 shows the analysis made through the comparison of the curves generated through speed and torque. As the result of various comparison with existing methodologies like PSO, Firefly and ANFIS we conclude that the method attains the improvement level in torque and reduces the ripple to maintain the stability of the system.

6. Conclusion

This paper presents a hybrid MFO-RNN calculation for the BLDCM drive framework. The proposed controller exhibits are tried under the MATLAB/simulink stage and compared with different procedures. The ideal parameters of speed controller and torque controller were acquired by the proposed procedures. Here the proposed control calculation depends on the improved MRPID controller for the speed and torque control circle. The proposed half and half MFO-RNN calculation was used to advance the pick up parameters of MRPID controller through the converter task. The exhibitions of framework parameters the speed, torque, back-EMF and current varieties do not exist. From the obtained result, the proposed hybrid MFO-ANN based MRPID controller provides an efficient solution for BLDCM framework by limiting the torque swell and settling times and providing an improvement in current profile due to its capacity than the existing procedures like ANFIS-FA and MFO-RNN utilizing FOPID controller individually. With enhanced and planned parameters, the final rotor configuration achieves a torque swell minimization which sets as a benchmark of this strategy.

References

- [1] Arunkumar and Thangavel, "A Review Paper on Torque Ripple Reduction and Power Quality Improvement in Brushless DC Motor Drives", An International Journal of International Electrical Engineering Journal (IEEJ), Vol.5, No.10, pp.1567-1575, 2014
- [2] Agand, Pedram, Mahdi Aliyari Shoorehdeli and Ali Khaki-Sedigh, "Adaptive recurrent neural network with Lyapunov stability learning rules for robot dynamic terms identification", An International Journal of Engineering Applications of Artificial Intelligence, Vol.65, pp.1-11, 2017
- [3] Alireza Shabaniyan, Armin Amini Poustchi Tousiwas, Massoud Pourmandi, Aminollah Khormali and Abdolhay Ataei, "Optimization of brushless direct current motor design using an intelligent technique", ISA Transactions, Vol.57, pp.311-321, 2015
- [4] Devendra Potnuru, K.Alice Mary and Saibabu Ch., "Design and implementation methodology for rapid control prototyping of closed loop speed control for BLDC motor", An International Journal of Electrical Systems and Information Technology, 2016
- [5] Cheng, Ming, Wei Hua, Jianzhong Zhang, and Wenxiang Zhao, "Overview of stator-permanent magnet brushless machines", IEEE Transactions on Industrial Electronics, Vol.58, No.11, pp.5087-5101, 2011
- [6] Dwari, Suman and Leila Parsa, "Fault-tolerant control of five-phase permanent-magnet motors with trapezoidal back EMF", IEEE Transactions on industrial electronics, Vol.58, No.2, pp.476-485, 2011
- [7] D.Das, N.Kumaresan, V.Nayanar, K.Navin Sam and N.Ammasai Gounden, "Development of BLDC Motor-Based Elevator System Suitable for DC Microgrid," IEEE/ASME Transactions on Mechatronics, Vol.21, No.3, pp.1552-1560, 2016
- [8] Gupta, R. A., Rajesh Kumar and Ajay Kumar Bansal, "Artificial intelligence applications in Permanent Magnet Brushless DC motor drives", An International Journal of Artificial Intelligence, Vol.33, No.3, pp.175-186, 2010
- [9] Guler, Nihal Fatma, Elif Derya Ubeyli and Inan

- Guler, "Recurrent neural networks employing Lyapunov exponents for EEG signals classification", *An International Journal of Expert systems with applications*, Vol.29, No.3, pp.506-514, 2005
- [10]
- [11]
- [12] Fang, Jiancheng, Haitao Li and Bangcheng Han, "Torque ripple reduction in BLDC torque motor with nonideal back EMF", *IEEE Transactions on power electronics*, Vol.27, No.11, pp.4630-4637, 2012
- [13] Jiancheng Fang, Xinxu Zhou and Gang Liu, "Precise Accelerated Torque Control for Small Inductance Brushless DC Motor", *IEEE Transactions On Power Electronics*, Vol. 28, No. 3, 2013
- [14] J.C. Gamazo-Real, E.Vazquez-Sanchez and J.Gomez-Gil, "Position and speed control of brushless DC motors using sensorless techniques and application trends", *An International Journal of Sensors*, Vol.10, No.7, pp. 6901-47, 2010
- [15] Joice, C. Sheeba, S. R. Paranjothi and V. Jawahar Senthil Kumar, "Digital control strategy for four quadrant operation of three phase BLDC motor with load variations", *IEEE Transactions on industrial informatics*, Vol.9, No.2, pp.974-982, 2013
- [16] H.E.A.Ibrahim, F.N.Hassan and Anas O.Shomer, "Optimal PID control of a brushless DC motor using PSO and BF techniques", *Ain Shams Engineering Journal*, Vol.5, pp.391-398, 2014
- [17] Jiancheng Fang, Xinxu Zhou and Gang Liu, "Instantaneous Torque Control of Small Inductance Brushless DC Motor", *IEEE Transactions on Power Electronics*, Vol.27, No.12, 2012
- [18] Kim and Ki-Chan, "A novel method for minimization of cogging torque and torque ripple for interior permanent magnet synchronous motor", *IEEE Transactions on Magnetics*, Vol.50, No.2, pp.793-796, 2014
- [19] Khan, M. Abdesh SK and M. Azizur Rahman, "A novel neuro-wavelet-based self-tuned wavelet controller for IPM motor drives", *IEEE Transactions on Industry Applications*, Vol.46, No.3, pp.1194-1203, 2010
- [20] Lee, Sun-Kwon, Gyu-Hong Kang, Jin Hur and Byoung-Woo Kim, "Stator and rotor shape designs of interior permanent magnet type brushless DC motor for

- reducing torque fluctuation", IEEE Transactions on Magnetics, Vol.48, No.11, pp.4662-4665, 2012
- [21] Lin, Yong-Kai and Yen-Shin Lai, "Pulsewidth modulation technique for BLDCM drives to reduce commutation torque ripple without calculation of commutation time", IEEE Transactions on industry applications, Vol.47, No.4, pp.1786-1793, 2011
- [22] Liu, Yong, Zi Qiang Zhu and David Howe, "Commutation-torque-ripple minimization in direct-torque-controlled PM brushless DC drives", IEEE Transactions on Industry Applications, Vol.43, No.4, pp.1012-1021, 2007
- [23] Kim, Ilhwan, Nobuaki Nakazawa, Sungsoo Kim, Chanwon Park and Chansu Yu, "Compensation of torque ripple in high performance BLDC motor drives", In international Journal of Control Engineering Practice, Vol.18, No.10, pp.1166-1172, 2010
- [24] R.Kumar and B.Singh, "Solar PV powered BLDC motor drive for water pumping using Cuk converter," IET Transactions of Electric Power Applications, Vol.11, No.2, pp.222-232, 2017
- [25] W.Li, J.Fang, H.Li and J.Tang, "Position
- [26] Mei, Rebecca Ng Shin, Mohd Herwan Sulaiman, Zuriani Mustaffa and Hamdan Daniyal, "Optimal reactive power dispatch solution by loss minimization using moth-flame optimization technique", An International Journal of Applied Soft Computing, Vol.59, pp.210-222, 2017
- [27] Mirjalili, Seyedali, "Moth-flame optimization algorithm: A novel nature-inspired heuristic paradigm", An International Journal of Knowledge-Based Systems, Vol.89, pp.228-249, 2015
- [28] Milivojevic, Nikola, Mahesh Krishnamurthy, Yusuf Gurkaynak, Anand Sathyan, Young-Joo Lee and Ali Emadi, "Stability analysis of FPGA-based control of brushless DC motors and generators using digital PWM technique", IEEE Transactions on industrial electronics, Vol.59, No.1, pp.343-351, 2012
- [29] Mohd Tariq, T.K.Bhattacharya, Nidhi Varshney and Dhilsha Rajapan, "Fast Response Antiwindup PI Speed Controller of Brushless DC Motor Drive: Modeling,

- Simulation and Implementation on DSP”, An International Journal of Electrical Systems and Information Technology, Vol.3, No.1, pp.1–13, 2016
- [30] Ozturk, Salih Baris, William C. Alexander and Hamid A. Toliyat, "Direct torque control of four-switch brushless DC motor with non-sinusoidal back EMF", IEEE Transactions on Power Electronics, Vol.25, No.2, pp.263-271, 2010
- [31] Parvez, Shahid and Zhiqiang Gao, "A wavelet-based multiresolution PID controller", IEEE Transactions on industry applications, Vol.41, No.2, pp.537-543, 2005
- [32] K.Premkumar and B.V.Manikandan, “Bat algorithm optimized fuzzy PD based speed controller for brushless direct current motor”, An International Journal of Engineering Science and Technology, Vol.19, No.2, pp.818-840, 2016
- [33] Shi, Jian and Tie-Cai Li, "New method to eliminate commutation torque ripple of brushless DC motor with minimum commutation time", IEEE Transactions on industrial electronics, Vol.60, No.6, pp.2139-2146, 2013
- [34] D.Suganyadevi and M.Sathiskumar, “Torque Ripple Minimization in BLDC Motor Using Four Switch Inverter”, An International Journal of Applications in Engineering and Technology, Vol.1, No.1, pp.20-25, 2015
- [35] S.A.KH.Mozaffari Niapour, M.Tabarraie and M.R.Feyzi, "A new robust speed-sensorless control strategy for high-performance brushless DC motor drives with reduced torque ripple", An International Journal of Control Engineering Practice, Vol.24, pp.42–54, 2014
- [36] R.Shanmugasundram, K.Muhammad Zakariah, and N.Yadaiah, “Implementation and Performance Analysis of Digital Controllers for Brushless DC Motor Drives”, IEEE/ASME Transactions on Mechatronics, Vol.19, No.1, 2014
- [37] Shi.T, Guo.Y, Song.P and Xia.C, “A new approach of minimizing commutation torque ripple for brushless DC motor based on DC–DC converter”, IEEE Transactions on Industrial Electronics, Vol.57, No.10, pp.3483-90, 2010

- [38] Sensorless Control Without Phase Shifter for High-Speed BLDC Motors With Low Inductance and Nonideal Back EMF," IEEE Transactions on Power Electronics, Vol.31, No.2, pp.1354-1366, 2016
- [39] Shi, Tingna, Yuntao Guo, Peng Song and Changliang Xia, "A new approach of minimizing commutation torque ripple for brushless DC motor based on DC-DC converter", IEEE Transactions on industrial electronics, Vol.57, No.10, pp.3483-3490, 2010
- [40] Xia, Changliang, Yingfa Wang and Tingna Shi, "Implementation of finite-state model predictive control for commutation torque ripple minimization of permanent-magnet brushless DC motor", IEEE Transactions on Industrial Electronics, Vol.60, No.3, pp.896-905, 2013
- [41] Xia, Changliang, Zhiqiang Li and Tingna Shi, "A control strategy for four-switch three-phase brushless DC motor using single current sensor", IEEE Transactions on industrial electronics, Vol.56, No.6, pp.2058-2066, 2009
- [42]